

ULRR

Conformational trimorphism in an ionic cocrystal of hesperetin

Item Type	Article
Authors	Jin, Shasha;Haskin, Molly M.;Andaloussi, Yassin H.;Ouyang, Ruiling;Gong, Junbo;Zaworotko, Michael
Citation	Crystal Growth & Design 2022 22 (11), 6390-6397
Publisher	American Chemical Society
Download date	2026-04-20 15:14:37
Item License	https://creativecommons.org/licenses/by-nc-sa/4.0/
Link to Item	https://doi.org/10.34961/researchrepository-ul.22700023

Conformational Trimorphism in an Ionic Cocrystal of Hesperetin

Shasha Jin, Molly M. Haskins, Yassin H. Andaloussi, Ruiling Ouyang, Junbo Gong,*
and Michael J. Zaworotko*Cite This: <https://doi.org/10.1021/acs.cgd.2c00861>

Read Online

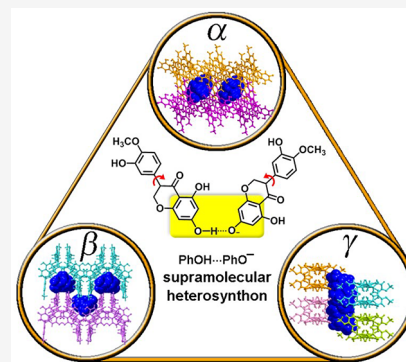
ACCESS |

Metrics & More

Article Recommendations

Supporting Information

ABSTRACT: We report the existence of conformational polymorphism in an ionic cocrystal (ICC) of the nutraceutical compound hesperetin (HES) in which its tetraethylammonium (TEA⁺) salt serves as a coformer. Three polymorphs, HESTE- α , HESTE- β and HESTE- γ , were characterized by single-crystal X-ray diffraction (SCXRD). Each polymorph was found to be sustained by phenol...phenolate supramolecular heterosynthons that self-assemble with phenol...phenol supramolecular homosynthons into C₃²(7) H-bonded motifs. Conformational variability in HES moieties and different relative orientations of the H-bonded motifs resulted in distinct crystal packing patterns: HESTE- α and HESTE- β exhibit H-bonded sheets; HESTE- γ is sustained by bilayers of H-bonded tapes. All three polymorphs were found to be stable upon exposure to humidity under accelerated stability conditions for 2 weeks. Under competitive slurry conditions, HESTE- α was observed to transform to the β or γ forms. Solvent selection impacted the relationship between HESTE- β (favored in EtOH) and HESTE- γ (favored in MeOH). A mixture of the β and γ forms was found to be present following H₂O slurry.



Crystalline forms of active pharmaceutical ingredients (APIs) are generally the preferred type of solid dosage forms in drug products because of their relative stability, ease of purification, and manufacturability when compared with corresponding amorphous forms.¹ Crystalline forms of drug molecules and other biologically active compounds, such as nutraceuticals^{2–4} and agrochemicals,⁵ can include polymorphs and multicomponent crystals such as salts, solvates (including hydrates), or cocrystals.^{6–13} Crystalline forms are relevant to oral drug delivery because they can influence physicochemical properties such as solubility and stability.¹⁴ Solid form screening,⁶ including high-throughput screening,¹⁵ to identify and characterize crystalline solid forms of drug molecules is therefore a key step during early drug development.¹⁶ The first step of solid form screening focuses upon identification of which compound should be selected for development, e.g. the neutral drug molecule, a pharmaceutically acceptable salt or a pharmaceutical cocrystal.^{17,18} Generally, the neutral (free acid or free base) form of a drug molecule would be preferred if it has suitable physicochemical properties, but the majority of new chemical entities being developed in the pharmaceutical industry exhibit low solubility,^{19,20} as defined by the Biopharmaceutical Classification System, BCS.²¹ Therefore, since polymorphs and hydrates tend not to offer significant changes in solubility,²² pharmaceutical salts^{23–25} and pharmaceutical cocrystals,^{26–30} which involve pharmaceutically acceptable salt or cocrystal formers, respectively, are typically then considered as possible lead candidates. Whereas cocrystals have long been known,³¹ their amenability to design

through crystal engineering approaches was not well recognized until the early 2000s when four papers detailed the design of pharmaceutical cocrystals.^{32–35} Successful crystal engineering approaches to cocrystal design are generally based on a knowledge of possible H-bonded supramolecular synthons.³⁶ In this context, H-bonded supramolecular heterosynthons³⁵ between coformers are key to understanding and designing cocrystals since their hierarchies^{37–42} can be used to project whether a cocrystal is amenable to being readily isolated.⁴³ Pharmaceutical cocrystals can significantly diversify the number of crystal forms available for a given API, thereby improving the likelihood that a crystalline form suitable for use in a drug product will be identified. Most importantly, pharmaceutical cocrystals can enhance the solubility of low solubility drug molecules to improve drug product performance.^{26,44} Molecular cocrystals (MCCs), which are cocrystals containing two or more nonvolatile neutral coformers in a stoichiometric ratio, have often been targeted when preparing pharmaceutical cocrystals.^{8,45} Ionic cocrystals⁴⁶ (ICCs) comprise at least one coformer that is a salt. Whereas both classes of cocrystals are typically sustained by H-bonds⁴⁷ or halogen bonds,⁴⁸ ICCs are almost always sustained by charge-assisted

Received: July 29, 2022

Revised: September 16, 2022

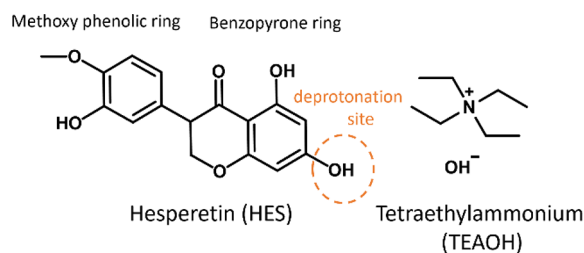
H-bonds, which are typically relatively strong in the context of H-bonds.⁴⁷ ICCs can also be based upon coordination bonds.^{49,50}

ICCs must have at least three components (cation + anion + neutral or ionic coformer) in the crystal lattice, i.e., A^+B^-C , where A^+ = cation, B^- = anion, and C = neutral coformer. ICCs therefore offer at least two variables that can be altered, which increases diversity in terms of composition and, therefore, properties. This contrasts with MCCs, which are typically composed of two molecular coformers, i.e., AB cocrystals. ICCs of general formula A^+B^-A or A^+B^-B , i.e., ICCs in which a free base or a free acid serves as the coformer with a salt of that base or acid, respectively, are also feasible. Such ICCs are of interest to pharmaceutical science since the active component of the ICC will represent a relatively high mass % of the resulting drug substance, which in turn results in a lower drug dosage. The marketed drug product Depakote is based upon a drug substance that is the ICC of valproic acid and sodium valproate and, therefore, exemplifies A^+B^-B drug substances.⁵¹ Other examples of A^+B^-A or A^+B^-B ICCs are presented in Table S1.

Investigation of the polymorphic behavior of an API is relevant to drug development since polymorphs can exhibit different physicochemical, mechanical, and biopharmaceutical properties.⁵² This means that regulatory bodies can require polymorphism studies,^{53,54} and there are strong commercial reasons for evaluating polymorphs since, in exceptional circumstances, the unexpected emergence of a more stable lower solubility polymorph can result in negative consequences, as exemplified by ritonavir (Norvir).⁵⁵ Compared to single-component crystals, systematic studies of polymorphism in cocrystals remain largely understudied even though increasing studies of cocrystals means that the number of polymorphic cocrystals has increased in recent years.⁵⁶ In this context, Aitipamula et al. concluded that the percentage of polymorphic cocrystals is comparable to the percentage of polymorphic single-component crystals on the basis of analysis of the Cambridge Structural Database (CSD).⁵⁶ In general, cocrystal polymorphs can be classified into synthon polymorphs,⁵⁷ conformational polymorphs,^{58,59} packing polymorphs, and tautomeric polymorphs.⁶⁰ Sometimes, cocrystal polymorphs may belong to two or more different classes. Most polymorphic studies on cocrystals reported MCCs exhibiting two^{61–63} or three^{64,65} polymorphic forms. There are only a few reports of dimorphic ICCs,⁶⁶ and even fewer that discuss trimorphic ICCs. Indeed, as far as we know, there is just one case of a trimorphic ICC, the ICC of lithium 4-methoxybenzoate with L-proline recently reported by our group.⁶⁷

In this contribution, we focus upon the nutraceutical hesperetin, HES (Scheme 1), which exhibits potentially useful biological properties such as antioxidant, anti-inflammatory, and antitumor activities,^{68,69} but offers relatively low solubility of $1.35 \text{ mg}\cdot\text{L}^{-1}$ ⁷⁰ and low bioavailability.^{71,72} HES belongs to the group of natural products known as flavonoids and contains multiple phenolic groups. Phenols are classified as medium strength H-bond donors³⁸ and have been established as being able to form supramolecular heterosynthons with H-bond acceptors such as chloride anions,³⁹ carboxylate moieties,⁴⁰ and aromatic nitrogen bases.⁴¹ Recently, we reported a crystal engineering study on ICCs of phenol and substituted phenol derivatives with their conjugate bases, which indicated that the phenol...phenolate ($\text{PhOH}\cdots\text{PhO}^-$)

Scheme 1. Molecular Structures and Abbreviations for the Cofomers Used Herein



supramolecular heterosynthon is robust and can be relied upon to form cocrystals.³⁷ We report herein on the synthesis and characterization of three polymorphs (α , β , γ) of the A^+B^-B type ICC formed between HES and its tetraethylammonium (TEA^+) salt, HESTEA.

HESTE A was prepared by slurring 150 mg (0.50 mmol) of HES and 186.6 μL (0.25 mmol) of 1.34 M tetraethylammonium hydroxide (TEAOH) in MeOH in 1 mL of MeOH, EtOH, or H_2O for 24 h. Recrystallization of the resulting bulk powder (shown to be HESTE A - α as determined by powder X-ray diffraction, PXRD) from MeOH via slow evaporation at room temperature afforded single crystals of HESTE A - α , as confirmed by single-crystal X-ray diffraction (SCXRD, see Supporting Information for experimental details). Liquid diffusion involving 1 mL of an EtOH solution of HESTE A powder layered below 2.3 mL of *n*-hexane yielded single crystals of HESTE A - β . HESTE A - γ was isolated by slow evaporation of 0.75 mL of an EtOH solution of 15 mg (0.050 mmol) of HES and 83.3 μL (0.025 mmol) of TEAOH in MeOH diluted to 0.3 M at RT. All three polymorphs were observed to be colorless and formed block-shaped crystals; relevant crystallographic parameters are presented in Table 1. Geometric parameters of the $\text{PhOH}\cdots\text{PhO}$ and $\text{PhOH}\cdots\text{PhOH}$ H-bonds in each polymorph are given in Table S2.

HES crystallized in the space group $P2_1/c$ with one molecule in the asymmetric unit. The crystal packing diagram is displayed in Figure S1, which reveals a chain of HES molecules connected through $\text{O}\cdots\text{H}\cdots\text{O}=\text{C}$ H-bonds [$2.6911(68) \text{ \AA}$].⁷³

HESTE A - α crystallized in the space group $P2_1/n$ with an asymmetric unit comprising one TEA^+ cation, one HES^- anion, and one HES molecule. The phenolate moiety of the HES^- anion forms H-bonds to a phenolic group on the benzopyrone ring from an adjacent HES molecule and a phenolic group on the methoxy phenolic ring from an HES^- anion via charge-assisted $\text{PhOH}\cdots\text{PhO}^-$ H-bonds [$\text{O}6\cdots\text{O}7^-$, $2.446(3) \text{ \AA}$; $\text{O}11\cdots\text{O}7^-$, $2.711(3) \text{ \AA}$, respectively]. Additionally, an HES molecule interacts with a phenolic group of a neighboring HES molecule via $\text{PhOH}\cdots\text{PhOH}$ H-bond [$\text{O}2\cdots\text{O}6$, $2.638(3) \text{ \AA}$], which results in a $\text{C}_3^2(7)$ H-bonded motif comprising one phenolate and three phenolic groups from two HES^- anions and two HES molecules, as illustrated in Figure 1a. When viewed down the *c*-axis, the $\text{C}_3^2(7)$ H-bonded motifs are organized in a “cross” shape and serve as nodes that are cross-linked by HES molecules and HES^- anions into H-bonded sheets. In these sheets, HES molecules form helical chains around 2-fold screw axes through $\text{PhOH}\cdots\text{PhOH}$ H-bonds that propagate along the *b*-axis while HES^- anions form zigzag chains through $\text{PhOH}\cdots\text{PhO}^-$ H-bonds that propagate along the *a*-axis (Figure 1b). HES or HES^- moieties from adjacent HES or HES^- chains align parallel between benzopyrone rings (highlighted in Figure 1b). Adjacent sheets

Table 1. Selected Crystallographic Data and Structure Refinement Parameters

compound abbreviation	HESTEA- α (TEA ⁺ HES ⁻)HES, α	HESTEA- β (TEA ⁺ HES ⁻)HES, β	HESTEA- γ (TEA ⁺ HES ⁻)HES, γ
formula		C ₄₀ H ₄₇ NO ₁₂	
crystal system	monoclinic	monoclinic	monoclinic
space group	<i>P</i> 2 ₁ / <i>n</i>	<i>P</i> 2 ₁ / <i>c</i>	<i>C</i> 2/ <i>c</i>
<i>a</i> (Å)	14.1323(5)	14.7566(9)	22.7154(7)
<i>b</i> (Å)	17.9440(7)	14.9419(10)	8.6532(3)
<i>c</i> (Å)	14.5214(4)	16.5652(11)	18.5287(6)
α (deg)	90	90	90
β (deg)	95.486(3)	95.328(2)	90.987(1)
γ (deg)	90	90	90
vol (Å ³)	3665.6(2)	3636.7(4)	3641.5(2)
density (g·cm ⁻³)	1.328	1.343	1.336
<i>Z</i> , <i>Z'</i>	4, 1	4, 1	4, 0.5
<i>T</i> (K)	135	135	135
<i>R</i> ₁	0.0770	0.0450	0.0520
w <i>R</i> ₂	0.1910	0.1142	0.1318
Goof	1.028	1.056	1.134
CCDC	2189972	2189975	2189977

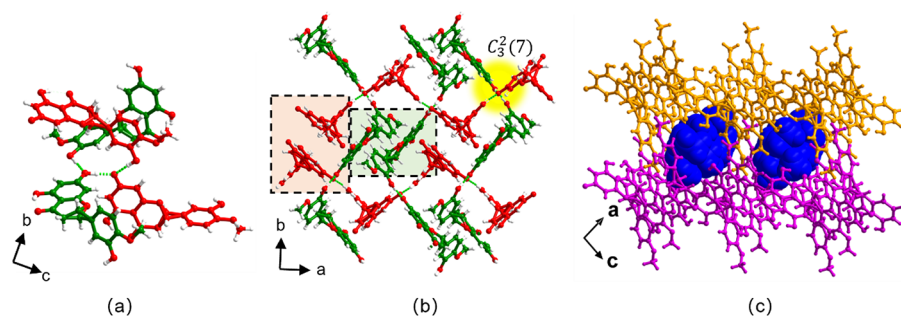


Figure 1. Crystal structure of HESTEA- α . HES molecules and HES⁻ anions are colored green and red, respectively. (a) The $C_3^2(7)$ H-bonded motif formed between phenolic and phenolate groups in HESTEA- α . (b) H-bonded sheets with HES moieties organized in zigzag chains along the *a* and *b* axes. (c) TEA⁺ cations (blue, space-filling mode) lie in pockets between H-bonded sheets. Cations are omitted for clarity in (a) and (b).

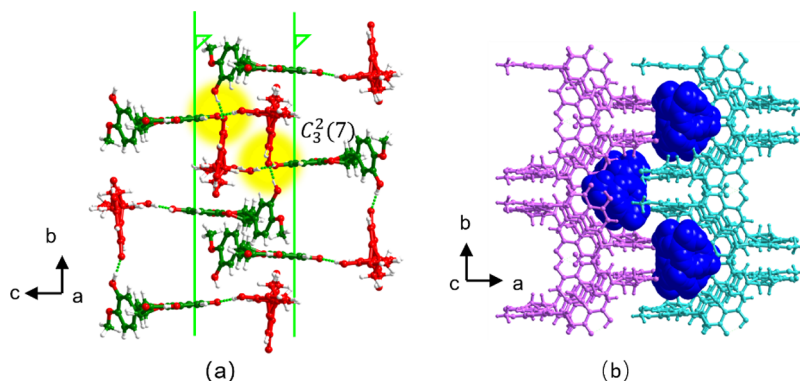


Figure 2. Crystal structure of HESTEA- β . HES molecules and HES⁻ anions are colored green and red, respectively. (a) Two helical chains around 2-fold screw axes interdigitate, thereby causing the formation of $C_3^2(7)$ H-bonded motifs (highlighted in yellow) sustained by two PhOH...PhO⁻ and one PhOH...PhOH H-bonds. Cations are omitted for clarity. (b) TEA⁺ cations (blue, space-filling mode) lie between H-bonded sheets.

stack via weak H-bonds in such a manner that square-pockets are generated, which contain TEA⁺ cations that are positioned via C–H...O and columbic forces (Figure 1c).

HESTEA- β crystallized in the space group *P*2₁/*c* with an asymmetric unit containing one TEA⁺ cation, one HES⁻ anion and one HES molecule. HES molecules and HES⁻ anions alternate and form a helical chain around a 2-fold screw axis sustained by PhOH...PhO⁻ [O2...O7, 2.6573(18) Å] and PhOH...PhOH [O11...O6, 2.6764(18) Å] H-bonds, which propagate along the *b*-axis (Figure 2a). Adjacent helical chains

interdigitate via PhOH...PhO⁻ [O6...O7̄, 2.4492(17) Å] H-bonds in such a manner that pairs of HES⁻ or HES are aligned antiparallel (Figure 2a). Like HESTEA- α , $C_3^2(7)$ H-bonded motifs are formed and comprise two PhOH...PhO⁻ and one PhOH...PhOH H-bonds between one phenolate and three phenolic groups. When viewed down the *a*-axis, the H-bonded motifs are once again organized in a “cross” shape, but HES and HES⁻ adopt a different orientation to that observed in HESTEA- α . When viewed down the *c*-axis, adjacent H-bonded sheets interdigitate with each other through weak H-bonds and

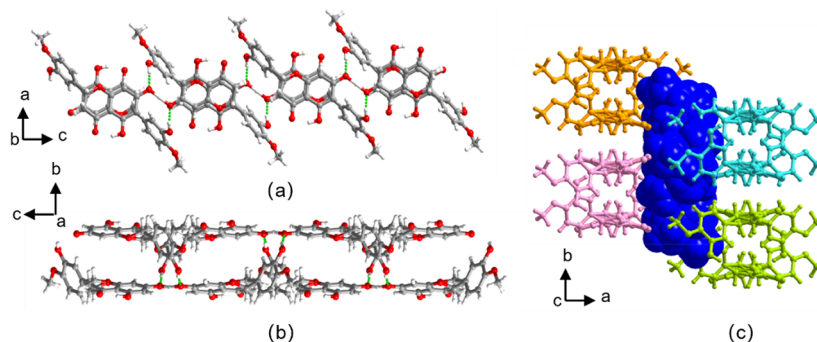


Figure 3. Crystal structure of HESTEA- γ . (a) $C_3^2(7)$ H-bonded motifs formed between phenolic and phenolate groups in HESTEA- γ assemble into a bilayer tape along the c -axis, as shown in (a) and (b) (cations omitted for clarity). (c) TEA⁺ cations (blue, space-filling mode) lie between the H-bonded tapes.

form cavities containing TEA⁺ cations that are engaged in C–H...O and columbic forces (Figure 2c).

HESTEA- γ crystallized in the space group $C2/c$ with an asymmetric unit comprising 0.5 of the chemical formula since TEA⁺ cations are disordered around an inversion center and an apparently symmetric H-bond between HES moieties enables the proton to sit at or close to a crystallographic 2-fold axis. The symmetric or close-to-symmetric nature of the [PhO...H...PhO[−]] anions is supported by the short O6...O6' distance of 2.4256(19) Å⁷⁴ and location of the proton from difference Fourier map inspection. In our recent work,³⁷ a CSD survey revealed that the average O...O[−] distance for PhOH...PhO[−] H-bonds is 2.528 ± 0.08 Å; the PhOH...PhO[−] H-bond in HESTEA- γ is shorter than the vast majority of previously reported structures. The classification of this PhOH...PhO[−] H-bond as symmetric or close-to-symmetric cannot be asserted using SCXRD, and further studies will be required in this context. As illustrated in Figure 3a, [PhO...H...PhO[−]] anions form H-bonds with two phenolic groups on the methoxy-substituted phenolic rings from two neighboring HES moieties [O2...O6, 2.663(2) Å], which forms a $C_3^2(7)$ motif (Figure 3a). In the H-bonded motifs, HES moieties align in an antiparallel face-to-face arrangement (4.363 Å between two benzopyrone rings), thereby forming a bilayer of tapes along the c -axis (Figure 3b). The bilayer of tapes stack around 2-fold rotation axes. The distance of adjacent tapes along the b -axis is 4.019 Å (between benzopyrone rings), while along the c -axis, TEA⁺ cations lie between adjacent tapes engaged in C–H...O and columbic forces (Figure 3c).

The experimental PXRD patterns of the HESTEA polymorphs are distinct from each other and match well with the corresponding calculated PXRD patterns (Figure S2). The relative orientation of the two HES moieties in the asymmetric units in HESTEA- α , - β , and - γ (Figure 4a–c) can be used to illustrate their different crystal packing patterns. HES molecules in HESTEA- α and HESTEA- β are arranged perpendicular in relation to the corresponding HES[−] anions, with dihedral angles (measured between benzopyrone ring planes from HES and HES[−]) of 88.94° and 76.92°, respectively. In HESTEA- γ the HES moieties are closer to planarity with a dihedral angle between two benzopyrone rings of 30.09°. Overall, the $C_3^2(7)$ H-bonded motifs in the three polymorphs (Scheme 2) differ in the relative orientation of the HES molecules and HES[−] anions. Conformational differences within the HES moieties become evident when their structures are overlaid (Figure 4d). As seen by aligning the methoxy phenolic moieties, the benzopyrone rings exhibit a high degree

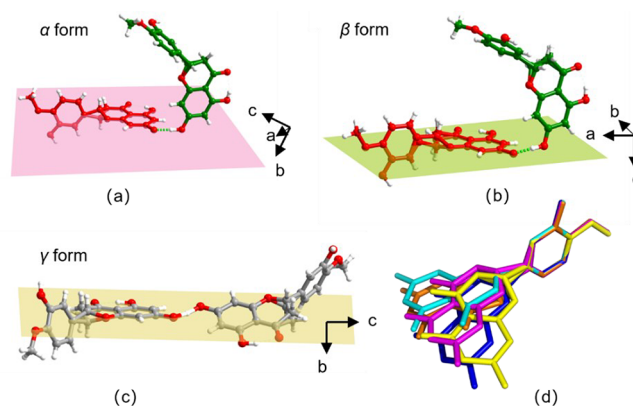
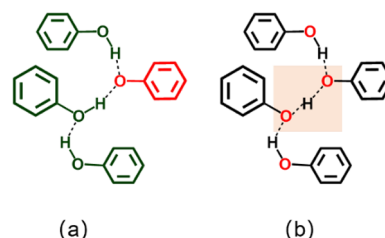


Figure 4. Relative orientation of HES moieties in the asymmetric units of (a) HESTEA- α , (b) HESTEA- β (HES molecules and anions are colored green and red, respectively), and (c) HESTEA- γ . (d) Overlay of the conformations of HES moieties in HESTEA- α (yellow for HES, blue for HES[−]), HESTEA- β (cyan for HES molecule, magenta for HES[−]), and HESTEA- γ (orange). Hydrogen atoms are omitted for clarity. Virtual planes through atoms on the benzopyrone rings are created in (a), (b), and (c). Chiral carbons are not included in plane calculations because they are disordered and nonplanar with other carbon atoms on the benzopyrone rings.

Scheme 2. Schematic Representation of (a) the $C_3^2(7)$ H-Bonded Motif Sustained By PhOH...PhO[−] and PhOH...PhO H-Bonds (Phenol, Green; Phenolate, Red) in HESTEA- α and - β and (b) the $C_3^2(7)$ H-Bonded Motif Comprising Symmetric H-Bond Found in HESTEA- γ



of torsional variability, but disorder of the chiral carbons means that torsion angles cannot be readily determined. In general, the conformational variability of HES moieties can be assessed through determination of the dihedral angles between the benzopyrone rings (chiral carbons excluded) and the methoxy phenolic rings of nonequivalent HES moieties. The equivalent dihedral angles of the seven HES entries in the CSD and the three HESTEA polymorphs reported herein are tabulated in

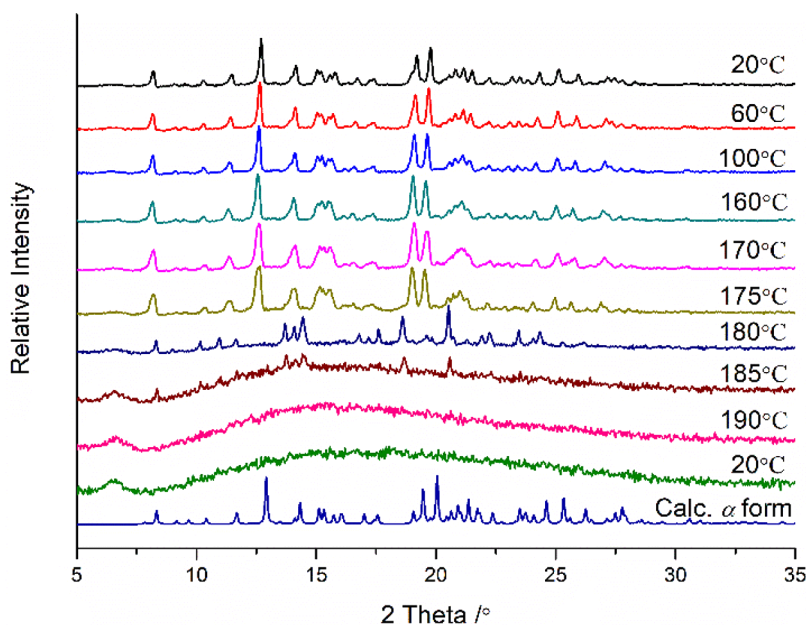


Figure 5. Variable temperature PXRD of HESTE- α (there is peak shift due to thermal expansion as ICC were collected at 135 K).

Table S3. In HES hydrate (FOYTOC),⁷⁵ the benzopyrone ring and the methoxy phenolic ring are almost parallel (3.69°). In HES cocrystals, HES moieties exhibit dihedral angles that range from 4.69° to 89.06° . This conformational variability is reflected in the HESTE ICC polymorphs reported herein, which may be classified as conformational polymorphs.^{58,60}

The thermal properties of the three HESTE polymorphs were investigated by means of thermogravimetric analysis (TGA), differential scanning calorimetry (DSC), and variable temperature powder X-ray diffraction (vt-PXRD). TGA data revealed that HESTE- α , - β , and - γ each decomposed at ca. 240°C , slightly lower than pure HES, which decomposed at ca. 260°C (Figure S3a). The DSC curve (Figure S3b) of HESTE- α displayed two endothermic events, the first being consistent with transformation to a new phase at ca. 182°C followed by a larger endotherm at ca. 193°C , which we attribute to melting. vt-PXRD data (Figure 5) also reveals a phase change by 180°C to a new crystal form with a different PXRD to that of any of the three polymorphs characterized by SCXRD. In contrast, heating of HESTE- β and HESTE- γ resulted in sharp melting endotherms at ca. 192 and 184°C , respectively, with vt-PXRD indicating that the β and γ polymorphs retained their structures until melting (Figure S4). All three HESTE polymorphs exhibit lower melting points than pure HES, which exhibited a single sharp melting endotherm at 232°C .

We also studied the relative stability of the HESTE polymorphs. When subjected to accelerated stability-testing conditions (40°C , 75% RH)⁷⁶ for 14 days, all three polymorphs retained stability (Figure S5). HESTE- α was initially obtained in bulk by slurring as described above. However, after HESTE- β and HESTE- γ were isolated, HESTE- α could not isolate using the same synthetic conditions. Rather, HESTE- β was thereafter obtained via slurring in EtOH, and HESTE- γ through slurring in MeOH or H_2O (see Supporting Information for details). These slurry experiments suggest that HESTE- α is less stable than β and γ .^{77,78} Table 2 and Figure S6 detail the relative stability of HESTE polymorphs as determined by competitive

Table 2. Results of Competitive Slurry

solvent	$\alpha + \beta$	$\beta + \gamma$	$\alpha + \gamma$
H_2O	β	$\gamma + \beta$	γ
MeOH	β	γ	γ
EtOH	β	β	γ

slurring of 1:1 mixtures of the α and β polymorphs, α and γ polymorphs, or β and γ polymorphs conducted in 1.5 mL of H_2O , MeOH, or EtOH. These competitive slurry experiments revealed that HESTE- α transformed into one of the other polymorphs in all three solvents. HESTE- β was found to be stable in EtOH, whereas HESTE- γ was isolated from MeOH, which correlates with the results of slurry synthesis. In the case of H_2O , even after 2 weeks the resulting powder remained a mixture. That HESTE- α is least stable is also suggested by its lower density^{79,80} ($1.328\text{ g}\cdot\text{cm}^{-3}$ at 135 K) versus β ($1.343\text{ g}\cdot\text{cm}^{-3}$) and γ ($1.336\text{ g}\cdot\text{cm}^{-3}$). HESTE- α might be classified as a disappearing polymorph^{77,78} since we have been unable to make it again despite repeated attempts (see experimental section of Supporting Information for details).

In conclusion, cocrystallization of HES and TEAOH afforded three polymorphs of the new ICC HESTE. SCXRD revealed that all polymorphs are sustained by $\text{PhOH}\cdots\text{PhO}^-$ and $\text{PhOH}\cdots\text{PhOH}$ H-bonds that assemble into $\text{C}_3^2(7)$ H-bonded motifs. We attribute the differences in crystal packing to conformational polymorphism. Competitive slurry experiments revealed the relative stability of HESTE polymorphs in an aqueous environment. The present study confirms the potential to apply crystal engineering to generate ICCs of phenolic compounds sustained by the $\text{PhOH}\cdots\text{PhO}^-$ supramolecular heterosynthon, which is persistent even when multiple polymorphs are possible since the polymorphism in HESTE can be attributed to conformational differences rather than different H-bonded motifs.

■ ASSOCIATED CONTENT

SI Supporting Information

The Supporting Information is available free of charge at <https://pubs.acs.org/doi/10.1021/acs.cgd.2c00861>.

Materials and methods, supporting figures, supporting tables (PDF)

Accession Codes

CCDC 2189972, 2189975, and 2189977 contain the supplementary crystallographic data for this paper. These data can be obtained free of charge via www.ccdc.cam.ac.uk/data_request/cif, or by emailing data_request@ccdc.cam.ac.uk, or by contacting The Cambridge Crystallographic Data Centre, 12 Union Road, Cambridge CB2 1EZ, UK; fax: +44 1223 336033.

■ AUTHOR INFORMATION

Corresponding Authors

Junbo Gong – State Key Laboratory of Chemical Engineering, School of Chemical Engineering and Technology, Tianjin University, Tianjin 300072, People's Republic of China; orcid.org/0000-0002-3376-3296; Email: xtal@ul.ie

Michael J. Zaworotko – Department of Chemical Sciences, Bernal Institute, University of Limerick, Limerick V94 T9PX, Ireland; orcid.org/0000-0002-1360-540X; Email: junbo_gong@tju.edu.cn

Authors

Shasha Jin – Department of Chemical Sciences, Bernal Institute, University of Limerick, Limerick V94 T9PX, Ireland

Molly M. Haskins – Department of Chemical Sciences, Bernal Institute, University of Limerick, Limerick V94 T9PX, Ireland

Yassin H. Andaloussi – Department of Chemical Sciences, Bernal Institute, University of Limerick, Limerick V94 T9PX, Ireland

Ruiling Ouyang – State Key Laboratory of Chemical Engineering, School of Chemical Engineering and Technology, Tianjin University, Tianjin 300072, People's Republic of China

Complete contact information is available at: <https://pubs.acs.org/doi/10.1021/acs.cgd.2c00861>

Notes

The authors declare no competing financial interest.

■ ACKNOWLEDGMENTS

The authors would like to thank Mr. Cheng-Hua Deng and Dr. Bai-Qiao Song for helpful discussions on crystal structure data collection and solution. The authors gratefully acknowledge Science Foundation Ireland (12/RC/2275_P2 and 16/IA/4624) for financial support.

■ REFERENCES

- (1) Allen, L. V.; Popovich, N. G.; Ansel, H. C. *Ansel's Pharmaceutical Dosage Forms and Drug Delivery Systems*; Lippincott Williams and Wilkins: Baltimore, MD, 2005.
- (2) Zhu, B.; Wang, J.-R.; Mei, X. Insight into the Phase Transformation among Various Solid Forms of Baicalein. *Cryst. Growth Des.* **2015**, *15*, 4959–4968.
- (3) Dima, C.; Assadpour, E.; Dima, S.; Jafari, S. M. Bioavailability of nutraceuticals: Role of the food matrix, processing conditions, the gastrointestinal tract, and nanodelivery systems. *Compr. Rev. Food Sci. Food Saf.* **2020**, *19*, 954–994.

- (4) Schultheiss, N.; Roe, M.; Boerrigter, S. X. M. Cocrystals of nutraceutical-p-coumaric acid with caffeine and theophylline: polymorphism and solid-state stability explored in detail using their crystal graphs. *CrystEngComm* **2011**, *13*, 611–619.

- (5) Lamberth, C.; Jeanmart, S.; Luksch, T.; Plant, A. Current Challenges and Trends in the Discovery of Agrochemicals. *Science* **2013**, *341*, 742–746.

- (6) Byrn, S.; Pfeiffer, R.; Ganey, M.; Hoiberg, C.; Poochikian, G. Pharmaceutical Solids: A Strategic Approach to Regulatory Considerations. *Pharm. Res.* **1995**, *12*, 945–954.

- (7) Berry, D. J.; Steed, J. W. Pharmaceutical cocrystals, salts and multicomponent systems; intermolecular interactions and property based design. *Adv. Drug. Delivery Rev.* **2017**, *117*, 3–24.

- (8) Aitipamula, S.; Banerjee, R.; Bansal, A. K.; Biradha, K.; Cheney, M. L.; Choudhury, A. R.; Desiraju, G. R.; Dikundwar, A. G.; Dubey, R.; Duggirala, N.; Ghogale, P. P.; Ghosh, S.; Goswami, P. K.; Goud, N. R.; Jetti, R. R. K. R.; Karpinski, P.; Kaushik, P.; Kumar, D.; Kumar, V.; Moulton, B.; Mukherjee, A.; Mukherjee, G.; Myerson, A. S.; Puri, V.; Ramanan, A.; Rajamannar, T.; Reddy, C. M.; Rodriguez-Hornedo, N.; Rogers, R. D.; Row, T. N. G.; Sanphui, P.; Shan, N.; Shete, G.; Singh, A.; Sun, C. C.; Swift, J. A.; Thaimattam, R.; Thakur, T. S.; Kumar Thaper, R.; Thomas, S. P.; Tothadi, S.; Wangala, V. R.; Variankaval, N.; Vishweshwar, P.; Weyna, D. R.; Zaworotko, M. J. Polymorphs, Salts, and Cocrystals: What's in a Name? *Cryst. Growth Des.* **2012**, *12*, 2147–2152.

- (9) Zhu, B.; Zhang, Q.; Wang, J.-R.; Mei, X. Cocrystals of Baicalein with Higher Solubility and Enhanced Bioavailability. *Cryst. Growth Des.* **2017**, *17*, 1893–1901.

- (10) Sanphui, P.; Goud, N. R.; Khandavilli, U. B. R.; Nangia, A. Fast Dissolving Curcumin Cocrystals. *Cryst. Growth Des.* **2011**, *11*, 4135–4145.

- (11) Smith, A. J.; Kavuru, P.; Arora, K. K.; Kesani, S.; Tan, J.; Zaworotko, M. J.; Shytle, R. D. Crystal engineering of green tea epigallocatechin-3-gallate (EGCG) cocrystals and pharmacokinetic modulation in rats. *Mol. Pharmaceutics* **2013**, *10*, 2948–2961.

- (12) Smith, A. J.; Kavuru, P.; Wojtas, L.; Zaworotko, M. J.; Shytle, R. D. Cocrystals of quercetin with improved solubility and oral bioavailability. *Mol. Pharmaceutics* **2011**, *8*, 1867–1876.

- (13) Khandavilli, U. B. R.; Skořepová, E.; Sinha, A. S.; Bhogala, B. R.; Maguire, N. M.; Maguire, A. R.; Lawrence, S. E. Cocrystals and a Salt of the Bioactive Flavonoid: Naringenin. *Cryst. Growth Des.* **2018**, *18*, 4571–4577.

- (14) Huang, L. F.; Tong, W. Q. Impact of solid state properties on developability assessment of drug candidates. *Adv. Drug Delivery Rev.* **2004**, *56*, 321–334.

- (15) Morissette, S. L.; Almarsson, O.; Peterson, M. L.; Remenar, J. F.; Read, M. J.; Lemmo, A. V.; Ellis, S.; Cima, M. J.; Gardner, C. R. High-throughput crystallization: polymorphs, salts, co-crystals and solvates of pharmaceutical solids. *Adv. Drug Delivery Rev.* **2004**, *56*, 275–300.

- (16) Aaltonen, J.; Alleso, M.; Mirza, S.; Koradia, V.; Gordon, K. C.; Rantanen, J. Solid form screening—a review. *Eur. J. Pharm. Biopharm.* **2009**, *71*, 23–37.

- (17) Sarma, B.; Chen, J.; Hsi, H.-Y.; Myerson, A. S. Solid forms of pharmaceuticals: polymorphs, salts and cocrystals. *Korean J. Chem. Eng.* **2011**, *28*, 315–322.

- (18) Ohannessian, L.; Streeter, A. J. *Handbook of Pharmaceutical Analysis*; Marcel Dekker, Inc., 2002.

- (19) Di, L.; Kerns, E. H.; Carter, G. T. Drug-Like Property Concepts in Pharmaceutical Design. *Curr. Pharm. Des.* **2009**, *15*, 2184–2194.

- (20) Fahr, A.; Liu, X. Drug Delivery Strategies for Poorly Water Soluble Drugs. *Expert Opin. Drug Delivery* **2007**, *4*, 403–416.

- (21) Amidon, G. L.; Lennernas, H.; Shah, V. P.; Crison, J. R. A Theoretical Basis for A Biopharmaceutical Drug Classification: the Correlation of in Vitro Drug Product and in Vivo Bioavailability. *Pharm. Res.* **1995**, *12*, 413–420.

- (22) Pudipeddi, M.; Serajuddin, A. T. M. Trends in Solubility of Polymorphs. *J. Pharm. Sci.* **2005**, *94*, 929–939.

- (23) Berge, S. M.; Bighley, L. D.; Monkhouse, D. C. Pharmaceutical Salts. *J. Pharm. Sci.* **1977**, *66*, 1–19.
- (24) Gould, P. L. Salt selection for basic drugs. *Int. J. Pharm.* **1986**, *33*, 201–217.
- (25) Morris, K. R.; Fakes, M. G.; Thakur, A. B.; Newman, A. W.; Singh, A. K.; Venit, J. J.; Spagnuolo, C. J.; Serajuddin, A. T. M. An integrated approach to the selection of optimal salt form for a new drug candidate. *Int. J. Pharm.* **1994**, *105*, 209–217.
- (26) Thakuria, R.; Delori, A.; Jones, W.; Lipert, M. P.; Roy, L.; Rodriguez-Hornedo, N. Pharmaceutical cocrystals and poorly soluble drugs. *Int. J. Pharm.* **2013**, *453*, 101–125.
- (27) Shan, N.; Zaworotko, M. J. The role of cocrystals in pharmaceutical science. *Drug Discovery Today*. **2008**, *13*, 440–446.
- (28) Schultheiss, N.; Newman, A. Pharmaceutical Cocrystals and Their Physicochemical Properties. *Cryst. Growth Des.* **2009**, *9*, 2950–2967.
- (29) Almarsson, O.; Zaworotko, M. J. Crystal engineering of the composition of pharmaceutical phases. Do pharmaceutical co-crystals represent a new path to improved medicines? *Chem. Commun.* **2004**, 1889–1896.
- (30) Bolla, G.; Nangia, A. Pharmaceutical cocrystals: walking the talk. *Chem. Commun.* **2016**, *52*, 8342–8360.
- (31) Stahly, G. P. A Survey of Cocrystals Reported Prior to 2000. *Cryst. Growth Des.* **2009**, *9*, 4212–4229.
- (32) Childs, S. L.; Chyall, L. J.; Dunlap, J. T.; Smolenskaya, V. N.; Stahly, B. C.; Stahly, G. P. Crystal Engineering Approach To Forming Cocrystals of Amine Hydrochlorides with Organic Acids. Molecular Complexes of Fluoxetine Hydrochloride with Benzoic, Succinic, and Fumaric Acids. *J. Am. Chem. Soc.* **2004**, *126*, 13335–13342.
- (33) Fleischman, S. G.; Kuduva, S. S.; McMahon, J. A.; Moulton, B.; Walsh, R. D. B.; Rodriguez-Hornedo, N.; Zaworotko, M. J. Crystal Engineering of the Composition of Pharmaceutical Phases: Multiple-Component Crystalline Solids Involving Carbamazepine. *Cryst. Growth Des.* **2003**, *3*, 909–919.
- (34) Remenar, J. F.; Morissette, S. L.; Peterson, M. L.; Moulton, B.; MacPhee, J. M.; Guzman, H. R.; Almarsson, O. Crystal Engineering of Novel Cocrystals of a Triazole Drug with 1,4-Dicarboxylic Acids. *J. Am. Chem. Soc.* **2003**, *125*, 8456–8457.
- (35) Walsh, R. D. B.; Bradner, M. W.; Fleischman, S.; Morales, L. A.; Moulton, B.; Rodríguez-Hornedo, N.; Zaworotko, M. J. Crystal engineering of the composition of pharmaceutical phases. *Chem. Commun.* **2003**, 186–187.
- (36) Desiraju, G. R. Supramolecular Synthons in Crystal Engineering—A New Organic Synthesis. *Angew. Chem., Int. Ed. Engl.* **1995**, *34*, 2311–2327.
- (37) Jin, S.; Sanii, R.; Song, B.-Q.; Zaworotko, M. J. Crystal Engineering of Ionic Cocrystals Sustained by the Phenol–Phenolate Supramolecular Heterosynthon. *Cryst. Growth Des.* **2022**, *22*, 4582–4591.
- (38) Haskins, M. M.; Lusi, M.; Zaworotko, M. J. Supramolecular Synthon Promiscuity in Phosphoric Acid-Dihydrogen Phosphate Ionic Cocrystals. *Cryst. Growth Des.* **2022**, *22*, 3333–3342.
- (39) Duggirala, N. K.; Wood, G. P. F.; Fischer, A.; Wojtas, L.; Perry, M. L.; Zaworotko, M. J. Persistent Phenol⋯Chloride Hydrogen Bonds in the Presence of Carboxylic Acid Moieties. *Cryst. Growth Des.* **2015**, *15*, 4341–4354.
- (40) Kavuru, P.; Aboarayas, D.; Arora, K. K.; Clarke, H. D.; Kennedy, A.; Marshall, L.; Ong, T. T.; Perman, J.; Pujari, T.; Wojtas, L.; Zaworotko, M. J. Persistent Hydrogen Bonds Between Carboxylates and Weakly Acidic Hydroxyl Moieties in Cocrystals of Zwitterions. *Cryst. Growth Des.* **2010**, *10*, 3568–3584.
- (41) Shattock, A. R.; Arora, K. K.; Vishweshwar, P.; Zaworotko, M. J. Persistent carboxylic acid–pyridine hydrogen bonds in cocrystals that also contain a hydroxyl moiety. *Cryst. Growth Des.* **2008**, *8*, 4533–4545.
- (42) Bis, J. A.; Vishweshwar, P.; Weyna, D.; Zaworotko, M. J. Persistent hydroxyl–pyridine hydrogen bonds in cocrystals that contain a cyano acceptor. *Mol. Pharmaceutics* **2007**, *4*, 401–416.
- (43) Bolla, G.; Sarma, B.; Nangia, A. K. Crystal Engineering of Pharmaceutical Cocrystals in the Discovery and Development of Improved Drugs. *Chem. Rev.* **2022**, *122*, 11514–11603.
- (44) Babu, N. J.; Nangia, A. Solubility Advantage of Amorphous Drugs and Pharmaceutical Cocrystals. *Cryst. Growth Des.* **2011**, *11*, 2662–2679.
- (45) Duggirala, N. K.; Perry, M. L.; Almarsson, O.; Zaworotko, M. J. Pharmaceutical cocrystals: along the path to improved medicines. *Chem. Commun.* **2016**, *52*, 640–655.
- (46) Braga, D.; Grepioni, F.; Maini, L.; Prosperi, S.; Gobetto, R.; Chierotti, M. R. From unexpected reactions to a new family of ionic co-crystals: the case of barbituric acid with alkali bromides and caesium iodide. *Chem. Commun.* **2010**, *46*, 7715–7717.
- (47) Bhattacharya, S. P. K. S.; Zaworotko, M. J. *The Role of Hydrogen Bonding in Co-Crystals*; The Royal Society of Chemistry, 2018.
- (48) Cavallo, G.; Metrangolo, P.; Milani, R.; Pilati, T.; Priimagi, A.; Resnati, G.; Terraneo, G. The Halogen Bond. *Chem. Rev.* **2016**, *116*, 2478–2601.
- (49) Duggirala, N. K.; Smith, A. J.; Wojtas, L.; Shytle, R. D.; Zaworotko, M. J. Physical Stability Enhancement and Pharmacokinetics of a Lithium Ionic Cocrystal with Glucose. *Cryst. Growth Des.* **2014**, *14*, 6135–6142.
- (50) Smith, A. J.; Kim, S. H.; Duggirala, N. K.; Jin, J.; Wojtas, L.; Ehrhart, J.; Giunta, B.; Tan, J.; Zaworotko, M. J.; Shytle, R. D. Improving lithium therapeutics by crystal engineering of novel ionic cocrystals. *Mol. Pharmaceutics* **2013**, *10*, 4728–4738.
- (51) Kavanagh, O. N.; Croker, D. M.; Walker, G. M.; Zaworotko, M. J. Pharmaceutical cocrystals: from serendipity to design to application. *Drug Discovery Today*. **2019**, *24*, 796–804.
- (52) Halebian, J.; Mccrone, W. Pharmaceutical applications of polymorphism. *J. Pharm. Sci.* **1969**, *58*, 911–929.
- (53) *FDA Guidance for Industry: ANDAs: Pharmaceutical Solid Polymorphism*; U.S. Food and Drug Administration, 2007.
- (54) *Guidance for Submitting Supporting Documentation in Drug Applications for the Manufacture of Drug Substances*; U.S. Food and Drug Administration, 1987.
- (55) Bauer, J.; Spanton, S.; Henry, R.; Quick, J.; Dziki, W.; Porter, W.; Morris, J. Ritonavir: An Extraordinary Example of Conformational Polymorphism. *Pharm. Res.* **2001**, *18*, 859–866.
- (56) Aitipamula, S.; Chow, P. S.; Tan, R. B. H. Polymorphs and Solvates of a Cocrystal Involving an Analgesic Drug, Ethenzamide, and 3,5-Dinitrobenzoic Acid. *Cryst. Growth Des.* **2010**, *10*, 2229–2238.
- (57) Mukherjee, A.; Desiraju, G. R. Synthon polymorphism and pseudopolymorphism in co-crystals. The 4,4'-bipyridine-4-hydroxybenzoic acid structural landscape. *Chem. Commun.* **2011**, *47*, 4090–4092.
- (58) Cruz-Cabeza, A. J.; Bernstein, J. Conformational polymorphism. *Chem. Rev.* **2014**, *114*, 2170–2191.
- (59) Nangia, A. Conformational Polymorphism in Organic Crystals. *Acc. Chem. Res.* **2008**, *41*, 595–604.
- (60) Aitipamula, S.; Chow, P. S.; Tan, R. B. H. Polymorphism in cocrystals: a review and assessment of its significance. *CrystEngComm* **2014**, *16*, 3451–3465.
- (61) Singaraju, A. B.; Bahl, D.; Wang, C.; Swenson, D. C.; Sun, C. C.; Stevens, L. L. Molecular Interpretation of the Compaction Performance and Mechanical Properties of Caffeine Cocrystals: A Polymorphic Study. *Mol. Pharmaceutics* **2020**, *17*, 21–31.
- (62) Mishra, M. K.; Mishra, K.; Narayan, A.; Reddy, C. M.; Vangala, V. R. Structural Basis for Mechanical Anisotropy in Polymorphs of a Caffeine–Glutaric Acid Cocrystal. *Cryst. Growth Des.* **2020**, *20*, 6306–6315.
- (63) Yan, Y.; Dai, X.-L.; Jia, J.-L.; Zhao, X.-H.; Li, Z.-W.; Lu, T.-B.; Chen, J.-M. Crystal Structures, Stability, and Solubility Evaluation of Two Polymorphs of a 2:1 Melatonin–Piperazine Cocrystal. *Cryst. Growth Des.* **2020**, *20*, 1079–1087.
- (64) Topic, F.; Lisac, K.; Arhangel'skis, M.; Rissanen, K.; Cincic, D.; Friscic, T. Cocrystal trimorphism as a consequence of the

orthogonality of halogen- and hydrogen-bonds synthons. *Chem. Commun.* **2019**, *55*, 14066–14069.

(65) Bolla, G.; Mittapalli, S.; Nangia, A. Celecoxib cocrystal polymorphs with cyclic amides: synthons of a sulfonamide drug with carboxamide coformers. *CrystEngComm* **2014**, *16*, 24–27.

(66) Marek, P. H.; Cichowicz, G.; Osowicka, D. M.; Madura, I. D.; Dobrzycki, Ł.; Cyrański, M. K.; Ciesielski, A. Polymorphism and structural diversities of LiClO₄-β-alanine ionic co-crystals. *CrystEngComm* **2020**, *22*, 4427–4437.

(67) Sanii, R.; Andaloussi, Y. H.; Patyk-Każmierczak, E.; Zaworotko, M. J. Polymorphism in Ionic Cocrystals Comprising Lithium Salts and L-Proline. *Cryst. Growth Des.* **2022**, *22*, 3786–3794.

(68) Yang, H. L.; Chen, S. C.; Senthil Kumar, K. J.; Yu, K. N.; Lee Chao, P. D.; Tsai, S. Y.; Hou, Y. C.; Hseu, Y. C. Antioxidant and anti-inflammatory potential of hesperetin metabolites obtained from hesperetin-administered rat serum: an ex vivo approach. *J. Agric. Food Chem.* **2012**, *60*, 522–532.

(69) Zarebczan, B.; Pinchot, S. N.; Kunnimalaiyaan, M.; Chen, H. Hesperetin, a potential therapy for carcinoid cancer. *Am. J. Surg.* **2011**, *201*, 329–333.

(70) Liu, L.; Chen, J. Solubility of Hesperetin in Various Solvents from (288.2 to 323.2) K. *J. Chem. Eng. Data* **2008**, *53*, 1649–1650.

(71) Krogholm, K. S.; Bredsdorff, L.; Knuthsen, P.; Haraldsdottir, J.; Rasmussen, S. E. Relative bioavailability of the flavonoids quercetin, hesperetin and naringenin given simultaneously through diet. *Eur. J. Clin. Nutr.* **2010**, *64*, 432–435.

(72) Kanaze, F. I.; Bounartzi, M. I.; Georganakis, M.; Niopas, I. Pharmacokinetics of the citrus flavanone aglycones hesperetin and naringenin after single oral administration in human subjects. *Eur. J. Clin. Nutr.* **2007**, *61*, 472–477.

(73) Fujii, S.; Yamagata, Y.; Jin, G.-Z.; Tomita, K.-i. Novel molecular conformation of (R,S) hesperetin in anhydrous crystal. *Chem. Pharm. Bull.* **1994**, *42*, 1143–1145.

(74) Kreevoy, M. M.; Marimanikkuppam, S.; Young, V. G.; Baran, J.; Szafran, M.; Schultz, A. J.; Trouw, F. Proton localization in hydrogen bonds: The Proton Potential Function and Dynamics in Sodium Hydrogen Bis(4-Nitrophenoxide) Dihydrate. *Ber. Bunsenges. Phys. Chem.* **1998**, *102*, 370–376.

(75) Shin, W.; Kim, S.; Chun, K. Structure of (R,S)-Hesperetin Monohydrate. *Acta Crystallogr.* **1987**, *C43*, 1946–1949.

(76) Huynh-Ba, K. *Handbook of Stability Testing in Pharmaceutical Development: Regulations, Methodologies, and Best Practices*; Springer: New York, 2008.

(77) Bucar, D. K.; Lancaster, R. W.; Bernstein, J. Disappearing polymorphs revisited. *Angew. Chem., Int. Ed.* **2015**, *54*, 6972–6993.

(78) Dunitz, J. D.; Bernstein, J. Disappearance Polymorphs. *Acc. Chem. Res.* **1995**, *28*, 193–200.

(79) Burger, A.; Ramberger, R. On the Polymorphism of Pharmaceuticals and Other Molecular Crystals. I. *Mikrochim. Acta* **1979**, *72*, 259–271.

(80) Burger, A.; Ramberger, R. On the Polymorphism of Pharmaceuticals and Other Molecular Crystals. II. *Mikrochim. Acta* **1979**, *72*, 273–316.